

# COMBINATORIAL CHARACTERIZATION OF COMPLEX POLYMERS: THIN FILM AND BIOMEDICAL POLYMERS

J. Carson Meredith<sup>\*1</sup>, Archie P. Smith<sup>1</sup>, Alex Tona<sup>2</sup>, Hoda Elgendy<sup>2</sup>, Alamgir Karim<sup>1</sup>, and Eric Amis<sup>1</sup>

<sup>1</sup>Polymers Division  
<sup>2</sup>Biotechnology Division  
National Institute of Standards and Technology  
100 Bureau Dr. Stop 8540  
Gaithersburg, MD 20899-8540

<sup>\*</sup>Current Address: School of Chemical Engineering  
Georgia Institute of Technology  
Atlanta, GA 30332-0100

## Introduction

Thin film polymers offer promise in applications including novel optical, electronic, and adhesive materials. Biodegradable polymers are of interest in tissue engineering, drug delivery, and degradable packaging. However, characterization of thin-film and biodegradable polymers is complex since many compositional and processing variables interact to produce desired optical, mechanical, surface chemistry and topography, and cell interaction properties. A need exists for more efficient methods to characterize complex thin-film and biodegradable polymer mixtures, composites, and cell-polymer systems.<sup>1</sup> Combinatorial methodologies, originally developed for pharmaceuticals, offer efficient measurement of chemical and physical properties over large regimes of variable space.<sup>1</sup> The primary limitation to characterizing polymers with combinatorial methods has been a shortage of techniques for preparing libraries with systematically varied composition ( $\phi$ ), thickness ( $h$ ), and temperature ( $T$ ). Recently the authors developed several new techniques for preparing polymer libraries containing continuous gradients in  $\phi$ ,  $h$ , and annealing  $T$ .<sup>2,3</sup> These high-throughput methods allow optimization of microstructure, chemistry, and cell interactions of tissue engineering biodegradable polymers, at an efficiency not attainable with conventional sample preparation and analytical methods. In this talk, combinatorial methods are presented for assaying thin-film phenomena<sup>2,4</sup> and cell adhesion and proliferation on biodegradable polymers as a function of composition, thickness, microstructure and topography of polymeric substrates.

## Experimental

**Materials.** All reagents were used without further purification. Polystyrene (PS),  $M_n=1,900$  g/mol,  $M_w/M_n=1.19$  was obtained from Goodyear.<sup>5</sup> Poly(D,L-lactide) (PDLA) was obtained from Alkermes (Medisorb 100DL, Lot #7248-345,  $M_n=127,000$  g/mol,  $M_w/M_n=1.56$ ) and poly( $\epsilon$ -caprolactone) (PCL) was obtained from Aldrich (Lot #07007DN,  $M_n=114,000$  g/mol  $M_w/M_n=1.43$ ). UMR-106 osteosarcoma cells and DMEM medium were obtained from ATCC. Streptomycin, penicillin, and amphotericin were obtained from Gibco.

**Preparation of Thickness Gradient Libraries.** A velocity-gradient knife coater<sup>2,4</sup> was developed to prepare coatings and thin films containing continuous thickness gradients. A 50  $\mu$ L drop of polymer solution (mass fraction 2 % to 5 %) was placed under a knife-edge with a stainless steel blade width of 2.5 cm, positioned at a height of 300  $\mu$ m and at a 5° angle with respect to the substrate. A computer-controlled motion stage (Parker Daedal) moves the substrate under the knife-edge at a constant acceleration, usually (0.5 to 1) mm/s<sup>2</sup>. This causes the substrate coating velocity to gradually increase from zero to a maximum value of (5 to 10) mm/s. The increase in fluid volume passing under the knife edge with increasing substrate velocity results in films with controllable thickness gradients. Thin film thickness-dependent phenomena can be investigated from nanometers to micrometers employing several  $h$ -gradient films with overlapping gradient ranges. We verified that the relatively weak thickness and temperature gradients do not induce appreciable flow in the polymer film over the experimental time scale.<sup>2,3</sup>

**Preparation of Composition Gradient Libraries.** Three steps are involved in preparing composition gradient films: gradient mixing, gradient deposition, and film spreading, described in detail elsewhere.<sup>2</sup> Gradient mixing utilizes two syringe pumps that introduce and withdraw polymer solutions (of

mass fraction  $x_A = x_B = 0.05$ ) to and from a small mixing vial at rates  $I$  and  $W$ , respectively. The infusion and withdrawal syringe pumps were started simultaneously under vigorous stirring of the vial solution, and a third syringe,  $S$ , was used to automatically extract solution from the vial. At the end of the sampling process, the sample syringe contained a solution of polymers A and B with a gradient in composition along the length of the syringe needle. However, the timescale for molecular diffusion is many orders of magnitude larger than the sampling time. The gradient solution is deposited as a thin stripe on the Si substrate and then spread as a film orthogonal to the composition gradient using a knife-edge coater.<sup>2,3</sup> After a few seconds most of the solvent evaporated, leaving behind a thin film with a gradient of polymer composition. The remaining solvent was removed under vacuum during annealing, described in the next section ( $T$ -gradient annealing). Since polymer melt diffusivities are typically about  $10^{-12}$  cm<sup>2</sup>/s, diffusion in the cast film can be neglected if the lengthscale resolved in measurements is significantly larger than the diffusion length,  $\sqrt{Dt}$ .

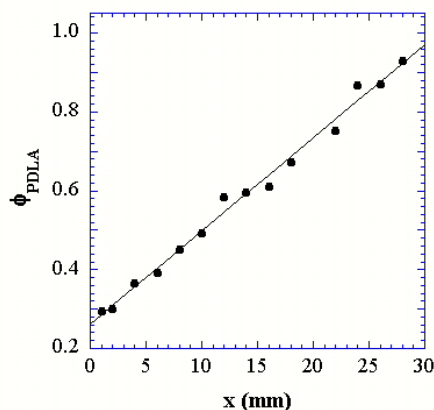


**Figure 1.** Composition (mass fraction) of PCL measured with FTIR spectroscopy on a continuous film  $\phi$ -gradient PDLA/PCL library.

FTIR spectra were measured with a Nicolet Magna 550 and were averaged 128 times at 4 cm<sup>-1</sup> resolution. The beam diameter, 500  $\mu$ m (approximate), was significantly larger than the diffusion length of 3  $\mu$ m (approximate) for the experimental timescale. Films (0.3 to 1)  $\mu$ m thick were coated on a sapphire substrate and a translation stage was used to obtain spectra at various positions on the continuous  $\phi$ -gradient. Compositions were measured with a standard uncertainty of mass fraction 4 % by calibration of peaks in the C-H stretch regime (2700 to 3100) cm<sup>-1</sup>. Figure 1 shows a typical composition gradient for a PDLA/PCL blend. Essentially linear gradients were obtained and the endpoints and slope agree with those predicted from mass balance.

**Temperature Gradient Annealing.** To explore a large  $T$  range, the  $\phi$ -gradient films were annealed on a  $T$ -gradient heating stage, with the  $T$ -gradient orthogonal to the  $\phi$ -gradient. This custom aluminum  $T$ -gradient stage uses a heat source and a heat sink to produce a linear gradient ranging between adjustable end-point temperatures. End-point temperatures typically range from (150  $\pm$  0.5) °C to (50.0  $\pm$  0.2) °C over 40 mm, but are adjustable within the limits of the heater, cooler, and maximum heat flow through the aluminum plate. To minimize oxidation and convective heat transfer from the substrate, the stage was sealed with an o-ring, glass plate, and vacuum pump. Each two-dimensional  $T$ - $\phi$  library contained about 3900 state points, respectively, where a "state point" is defined by the  $T$  and  $\phi$  variation over the area of a 200X optical microscope image:  $\Delta T = 0.5$  °C and  $\Delta \phi = 0.02$ .

## Results and Discussion

**Thin-Film Phenomena.** Figure 2 shows a composite of optical microscope images of a  $T$ - $h$  library of PS ( $M_n = 1900$  g/mol) on a SiO<sub>2</sub>/SiOH substrate.<sup>3</sup> The thickness ranges from (33 to 90) nm according to  $h = 33.1x^{0.30}$  (1 <  $x$  < 28) mm and 85 °C <  $T$  < 135 °C. The images, taken 2 h after initiation of dewetting, show wetted and dewetted regimes that are visible as dark and bright regions, respectively, to the unaided eye. Repeated examination of

combinatorial  $T$ - $h$  libraries at thicknesses ranging from (16 to 90) nm indicates three distinct thickness regimes with different hole nucleation mechanisms. For  $h > 55 \pm 4$  nm, discrete circular holes in the film nucleate via heterogeneities (e.g., dust) and grow at a rate dependent on  $T$ . The evolution of dewetted hole area,  $A$ , with time follows a universal exponential profile at all  $T$  and  $h$  observed in this regime.<sup>3</sup>

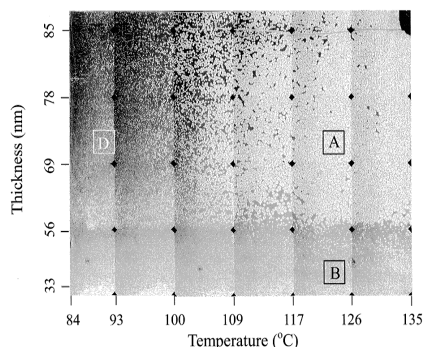


**Figure 2.** Composite of optical images of a  $T$ - $h$  combinatorial library of PS ( $M_w = 1800$  g/mol) on silicon,  $t = 2$  h, scale bar =  $(2.0 \pm 0.1)$  mm. Adapted with permission from ref. (3).

Below  $h \leq 55 \pm 4$  nm, there is a sharp and temperature independent transition to a regime where irregular, asymmetrical holes nucleate and grow more slowly than at  $h > 55$  nm. In the regime ( $33 < h < 55$ ) nm, the heterogeneous and capillary instability nucleation mechanisms compete. The asymmetrical holes present in this regime are surrounded by bicontinuous undulations in the film surface, with a characteristic spacing of  $7 \mu\text{m}$ , as indicated by optical microscopy.<sup>3</sup> AFM indicates a roughened surface with correlated surface undulations. A similar structure consisting of asymmetrical holes that break up into a bicontinuous pattern at late stage, termed an “intermediate morphology”, has been observed recently for 12 nm thick films of poly(styrene-*ran*-acrylonitrile).<sup>6</sup> Below  $h \sim 33$  nm, another transition in structure and nucleation is apparent. Here, holes are nucleated by capillary instability and grow more quickly than in the region  $33 \text{ nm} < h < 55$  nm.

Gradients in  $h$  of symmetric polystyrene-*b*-poly(methyl methacrylate) (PS-*b*-PMMA) with three different molecular masses were produced using the knife-edge flow coating technique described above.<sup>4</sup> After characterization of  $h$  with UV-visible interferometry, the films were annealed at  $170^\circ\text{C}$  for up to 30 h to allow lamellar organization. The resulting morphologies were characterized with optical microscopy (OM) and AFM. Three unique phenomena for block-copolymer segregation were observed: a wide thickness regime where smooth films form, the formation of bicontinuous morphologies, and a scaling law indicating a decrease in lateral bicontinuous size scale,  $\lambda$ , with increasing  $M_r$ ,  $\lambda \sim M_r^{-1.5}$ .

**Cell-Biodegradable Polymer Assays.** Each  $T$ - $\phi$  combinatorial library consists of a polymer coating on a clean silicon wafer,  $26 \times 30 \text{ mm}^2$ , with orthogonal and continuous gradients in blend composition,  $\phi_{\text{PCL}}$ , and annealing  $T$ . Composition,  $\phi_{\text{PCL}}$ , gradient films are placed on the  $T$ -gradient stage, with the  $\phi$ -gradient orthogonal to the  $T$ -gradient to produce two-dimensional  $T$ - $\phi_{\text{PCL}}$  libraries. PDLA/PCL blends are ideal for testing the effects of  $T$  and  $\phi$  on cell-polymer interactions, since this blend exhibits a lower critical solution temperature (LCST) that can be used to adjust microstructure and topography.<sup>7</sup>

UMR-106 cells were cultured on annealed  $T$ - $\phi_{\text{PCL}}$  libraries for periods of 1 d and 5 d in DMEM medium (ATCC) supplemented with 10 % fetal bovine serum, 100  $\mu\text{g/mL}$  streptomycin (Gibco), 100 units/mL penicillin (Gibco), and 0.25  $\mu\text{g/mL}$  amphotericin B (Gibco) at  $37^\circ\text{C}$  and 5 %  $\text{CO}_2$ . At termination, cultures were washed 3 times with 1 mL of phosphate buffered saline (PBS), and were fixed in volume fraction 3 % formaldehyde in PBS at  $4^\circ\text{C}$  for 5 min. To assay cell proliferation and differentiation of osteoblast phenotype, cells were stained for alkaline phosphatase (AIP) (Sigma kit 86-C). Figure 2 shows a  $T$ - $\phi$  library after 5 d culture, in which AIP is preferentially expressed by cells at  $T$  and  $\phi$  conditions near or within the polymer blend two-phase regime (white curve). In contrast, cells cultured concurrently at the same conditions on

Thermanox slides (Figure 2) show uniform adhesion and AIP expression. AFM indicates that the regions of preferred AIP expression have surface features averaging  $0.5 \pm 0.2 \mu\text{m}$  in height. Cells did not adhere or proliferate as well in areas with topographical features larger than  $0.7 \mu\text{m}$ , smaller than  $0.3 \mu\text{m}$ , or with mass fraction  $\phi_{\text{PCL}} > 0.5$ . These results also compare favorably to cultures performed on uniform PDLA/PCL controls. UMR-106 cells preferentially adhere and express AIP, a phenotype indicator for osteoblasts, within the LCST two-phase regime of the PDLA/PCL blend. Tentatively, we assign this behavior to cell sensitivity to topography and chemical differences between PDLA and PCL.

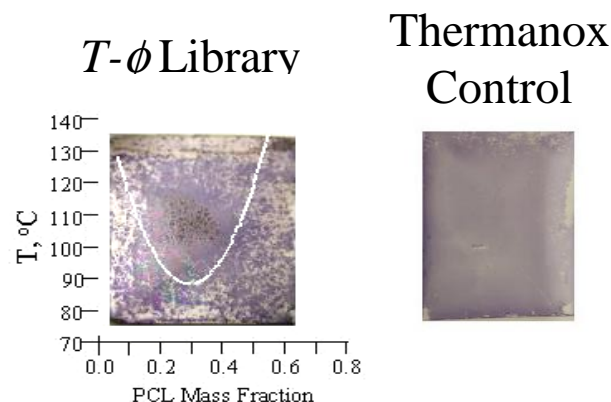


**Figure 3.** Left: An AIP stained  $T$ - $\phi$  library after 5 d culture with UMR-106 cells, showing preferentially AIP expression within the PDLA/PCL two-phase LCST regime. Right: AIP stained Thermanox control slide after 5 d culture with UMR-106 cells under the same conditions as left image.

## Conclusions

The combinatorial library techniques presented here allow rapid, efficient, and accurate exploration of the effects of polymer composition, thickness, and temperature on dewetting and segregation in thin polymer films, and on cell adhesion and proliferation on biodegradable polymers.

**Acknowledgements.** Support from the NIST Advanced Technology Program and the National Research Council (J.C.M.) is acknowledged.

## References

- (1) Brocchini, S.; James, K.; Tangpasuthadol, V.; Kohn, J. J. *Biomed. Mater. Res.* **1998**, *42*, 66.
- (2) Meredith, J. C.; Karim, A.; Amis, E. J. *Macromolecules* **2000**, *33*, 5760-5762.
- (3) Meredith, J. C.; Smith, A. P.; Karim, A.; Amis, E. J. *Macromolecules* **2000**, in press.
- (4) Smith, A. P.; Meredith, J. C.; Douglas, J.; Karim, A.; Amis, E. J., *Phys. Rev. Lett.*, **2000**, submitted.
- (5) Certain equipment and instruments or materials are identified in the paper in order to adequately specify the experimental details. Such identification does not imply recommendation by the National Institute of Standards and Technology, nor does it imply the materials are necessarily the best available for the purpose.
- (6) Masson, J. L.; Green, P. F., *J. Chem. Phys.* **1999**, *112*, 349.
- (7) Meredith, J. C.; Amis, E. J., *Macromol. Chem. Phys.* **2000**, *200*, 733-739.